Supporting Information

Tuning the transport and magnetism in Cr-Bi_2Se_3 Topological Insulator by Sb doping†

Y. Tung[a,*], C. W. Chong[a,*], C. W. Liao[a], C. H. Chang[a], S. Y. Huang[a], P. Y. Chuang[a], M. K. Lee[b], C. M. Cheng[c], Y. C. Li[d], C. P. Liu[d], and J. C. A. Huang[a,e,f]

[a]*Department of Physics, National Cheng Kung University, Tainan 70101, Taiwan.*
[b]*NSC Instrument Center at NCKU, Tainan 70101, Taiwan.*
[c]*National Synchrotron Radiation Research Center, Hsinchu 300, Taiwan.*
[d]*Department of Materials Science and Engineering, National Cheng Kung University, Tainan 70101, Taiwan.*
[e]*Advanced Optoelectronic Technology Center (AOTC), National Cheng Kung University Tainan 70101, Taiwan.*
[f]*Taiwan Consortium of Emergent Crystalline Materials (TCECM), Ministry of Science and Technology, Taipei 10622, Taiwan.*

* Y. Tung and C. W. Chong contributed equally to this work.
Email: cheongwei2000@yahoo.com and jcahuang@mail.ncku.edu.tw
† Electronic Supplementary Information (ESI)

Figure S1

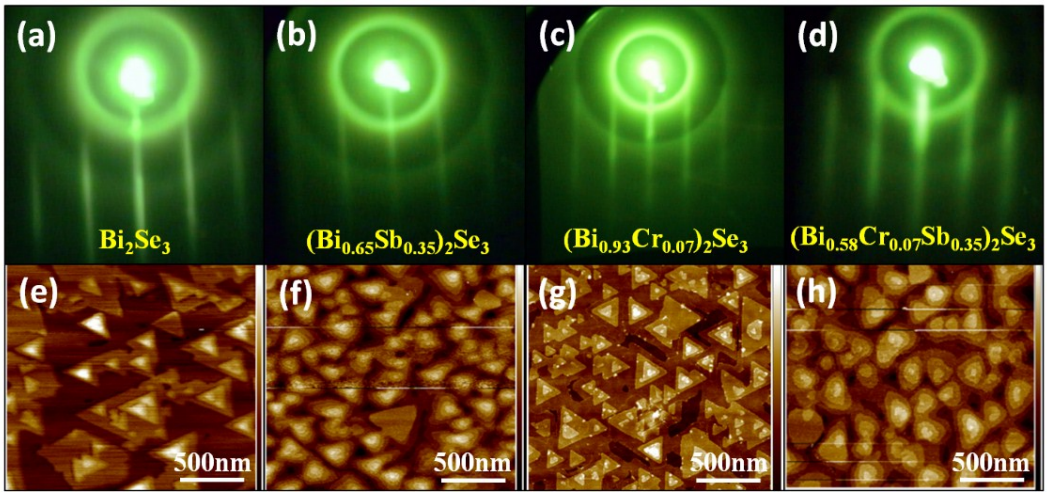

Figure S1 (a)-(d) display the RHEED pattern of various samples and (e)-(h) show the corresponding surface morphology that was analyzed by AFM. Without Cr

and Sb doping, the Bi_2Se_3 shows normal scale terraces. The surface of each films consists of characteristic triangular-shaped terraces and each roughness is around 1nm, reflecting the crystal structure still remains a fully tradition appearance of Bi_2Se_3. The width of the terraces decreases with increasing the doping of Sb and Cr. While codoped Sb and Cr samples exhibit surface roughness R_q ~0.912 nm. The obvious reduction of terrace width may indicate the evidence of Cr and Sb substitution into Bi site.

Figure S2

Sheet resistance R_s measured at 2K using physical property measurement system (PPMS).

x in Cr-doped $(Bi_{1-x}Sb_x)_2Se_3$	R_s (Ohm)	$k_F l$
0	1478.3	~17
0.35	13715.9	~2

Figure S3

Fitting of MC curves using Hikami-Larkin-Nagoka formula:

$$\Delta\sigma = \alpha\frac{e^2}{\pi h}\left[\Psi\left(\frac{1}{2}+\frac{B_\varphi}{B}\right) - \ln\left(\frac{B_\varphi}{B}\right)\right]$$

where α is a coefficient indicating the type of localization (α is positive for weak localization and negative for weak anti-localization), ψ is digamma function, and $B_\varphi = \hbar/4el_\varphi^2$ is characteristic field with $l_\varphi = (D\tau_\varphi)^{1/2}$ is the phase coherent length, τ_φ is the phase coherent time and D is diffusion constant.

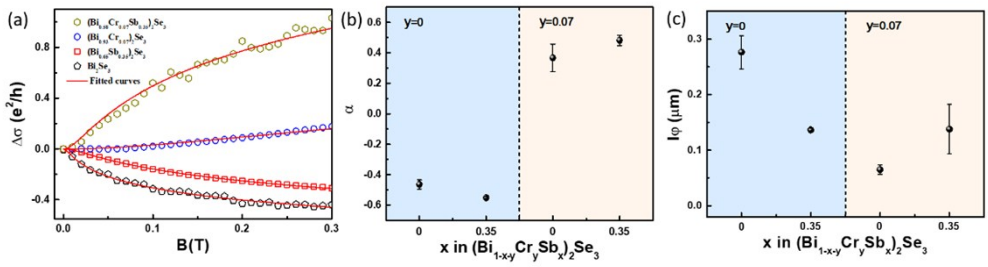

Figure S3 (a) The MC curves of Bi_2Se_3, $(Bi_{0.65}Sb_{0.35})_2Se_3$, $(Bi_{0.93}Cr_{0.07})_2Se_3$ and $(Bi_{0.58}Cr_{0.07}Sb_{0.35})_2Se_3$ are fitted with HLN equation; (b) & (c) illustrate the extracted α and lφ.

Figure S4

The out-of-plane magnetic properties of (Cr, Bi)$_2$Se$_3$ (Cr-BS) and Sb-doped (Cr, Bi)$_2$Se$_3$ (Cr-BSS) were measured by SQUID magnetometer at 2K. It's difficult to resolve the magnetic signal owing to the small amount of Cr doping level (y=0.07), Thus, for this SQUID measurement, we used thicker sample (80 QLs) with higher Cr concentration than that shown in the manuscript.

As shown in Fig. S4, both Cr-BS and Cr-BSS exhibit nonlinear magnetization as a function of magnetic fields. However, Sb-doped Cr-BS clearly presents significant larger magnetic moment than that of non-Sb-doped case. Such nonlinear curve reveals similar features as AHE, which confirms the non-linear Hall effect indeed induced by the magnetism.

Although the used samples are different from those in the manuscript, with this experiments, we demonstrate the positive role of Sb-doping in enhancing the magnetism in Cr-BS at a fix Cr content.

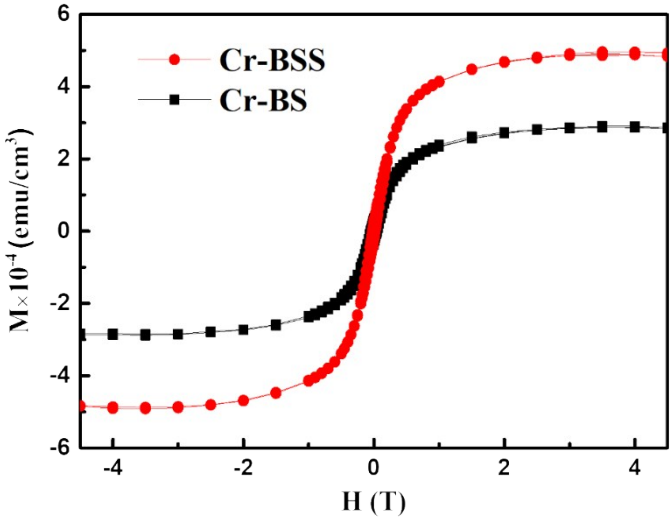

Figure S4 M-H loop of the 80QL (Cr, Bi)$_2$Se$_3$ and Sb-doped (Cr, Bi)$_2$Se$_3$ measured at B-field applied perpendicular to sample plane at 2K.